Effective stimulated laser cooling of atoms with a three-level Λ configuration by two negatively detuned standing light waves

Michael Drewsen*
Institute of Physics and Astronomy, Aarhus University, 8000 Aarhus C, Denmark
(Received 18 March 1994; revised manuscript received 17 August 1994)

A laser cooling scheme for atoms with an effective three-level Λ configuration is presented. The cooling force is obtained by using two standing light waves, each interacting only with one of the two atomic transitions and both detuned red with respect to the transition. For a given laser power, the force exceeds the largest force on a two-level atom by a factor of 2 or more and the atomic velocity capture range is at the same time significantly increased. The spatially averaged force as well as the spatially averaged momentum diffusion coefficient, as a function of the atomic velocity, is calculated. The semiclassical steady-state momentum distributions are presented for some specific cases and an experimental realization of the cooling scheme is proposed for the case of metastable helium.

PACS number(s): 32.80.Pj, 42.50.Vk

I. INTRODUCTION

Manipulation of multilevel atoms by laser light has been studied both theoretically and experimentally during the past decade [1–7]. The qualitative new physics that is generally connected with these multilevel systems as compared to two-level situations has offered many new possibilities in laser cooling. For low laser intensities, polarization gradient laser cooling [1] has made it possible to reach temperatures much below the Doppler limit [8], which is the temperature limit for two-level atoms in optical molasses. Laser cooling of three-level atoms by standing light waves has recently also produced temperatures below the Doppler limit [2,3]. Coherent population trapping [4], where atoms in a random walk by chance fall into a coherent superposition state that does not interact with the light field, can give rise to very narrow structures in the atomic momentum distribution. For high laser intensities, nonzero forces on stationary three-level atoms in standing light waves have been suggested and observed [5]. Also coherent atomic beam splitters utilizing three-level atoms have been considered lately [6].

In the present paper, the situation of a three-level atom with a Λ configuration moving in two standing light waves, each interacting only with one of the two transitions, will be discussed. The general formalism given in [9] is applied to calculate the force acting on the atom and the momentum diffusion coefficient for such a three-level case. The emphasis will be on situations where strong cooling forces and large velocity capture ranges can be obtained at the same time. Such schemes could represent alternatives to proposed laser-cooling schemes with the same characteristics [10,11], when an effective Λ configuration is present in the atoms of interest.

*Permanent address: Fakultät für Physik, Universität Konstanz, D-78434 Konstanz, Germany.

II. THE FORCE AND THE MOMENTUM DIFFUSION COEFFICIENT

The general character of the discussion in [9] makes it straightforward in principle to calculate the force F and the momentum diffusion coefficient D for multilevel atoms moving in light fields. The main difference from the two-level case discussed in [9] lies in the differences in the equation of motion of the internal-state density matrix and hence in the operators used for calculating F and D.

In Fig. 1 a three-level Λ system is shown where Γ_{ab} and Γ_{cb} represent the decay rates of the excited state $|b\rangle$ toward the stable states $|a\rangle$ and $|c\rangle$, respectively. If the atom is assumed to interact with two standing waves along the z axis which have a relative displacement of the nodes of Δz with respect to each other and where the one wave only couples the $|a\rangle$ and $|b\rangle$ states with a maximum Rabi frequency of κ_{ab}, while the other only couples the $|c\rangle$ and $|b\rangle$ states with a maximum Rabi frequency of κ_{cb}, then the interaction part of the Hamiltonian in the rotating-wave approximation (RWA) reads

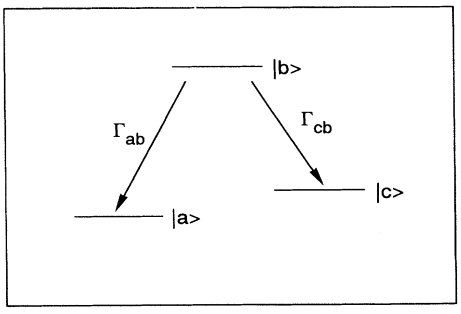

FIG. 1. Sketch of a three-level Λ system. Γ_{ab} and Γ_{cb} represent the decay rate of the state $|b\rangle$ to the states $|a\rangle$ and $|c\rangle$, respectively.

$$V_{AL}=-\tfrac{1}{2}[\kappa_{ab}\cos(kz)(|a\rangle\langle b|+|b\rangle\langle a|) +\kappa_{cb}\cos(kz+\phi)(|c\rangle\langle b|+|b\rangle\langle c|)] . \quad (1)$$

Here k is the norm of the wave vectors (assumed to be the same for both standing waves) and $\phi\equiv k\Delta z$. The equations necessary for calculating the spatial and the velocity-dependent force $F(z,v)$ and the momentum diffusion coefficient $D(z,v)$ are, for this situation, presented in the Appendix.

To limit the discussion, the spatially averaged values of the force $\bar{F}$ and the momentum diffusion coefficient $\bar{D}$ given by

$$\bar{F}(v)=\int F(z,v)dz \quad (2)$$

and

$$\bar{D}(v)=\int D(z,v)dz \quad (3)$$

will only be considered in the following. By varying the Rabi frequencies κ_{ab} and κ_{cb}, the phase ϕ, the detunings δ_{ab} and δ_{cb} (defined as the laser frequency minus the transition frequencies) as well as the ratio between the decay rates, a variety of different shapes of $\bar{F}$ and $\bar{D}$ as a function of velocity can be obtained. In the following a special situation, which is very interesting for laser cooling of atoms from both a theoretical and an experimental point of view, will be considered.

A. The mean force $\bar{F}$

In Fig. 2 the force $\bar{F}$ is shown (solid curve) for the Λ system with $\Gamma_{ab}=\Gamma_{cb}=\Gamma$, $\kappa_{ab}=40\Gamma$, $\kappa_{cb}=4\Gamma$, $\delta_{ab}=-2\Gamma$, $\delta_{cb}=-20\Gamma$, and $\phi=0$. The force exhibits several important features for laser cooling. First, the force is an odd function of v, as needed for cooling toward zero velocity. Second, it has a constant sign in the entire positive velocity range, i.e., the velocity range from which this force can capture atoms is in principle infinite, in contrast to stimulated cooling of two-level atoms [12]. Third, the range where the force exceeds the maximum Doppler-cooling force ($-\frac{1}{2}\hbar k\Gamma$) is nearly an order of magnitude larger than for the best two-level case with the same laser intensity. Fourth, the maximum force is nearly twice as large as the maximum obtainable one with the same laser intensity in a two-level situation. The last two features will reduce the cooling time needed in experiments.

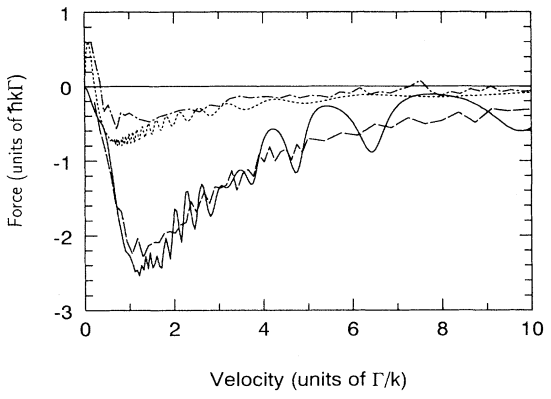

FIG. 2. Spatially averaged force acting on an atom in standing light fields. Solid curve: the force $\bar{F}$ for a Λ-system case with $\Gamma_{ab}=\Gamma_{cb}=\Gamma$, $\kappa_{ab}=40\Gamma$, $\kappa_{cb}=4\Gamma$, $\delta_{ab}=-2\Gamma$, $\delta_{cb}=-20\Gamma$, and $\phi=0$. Dashed curve: dressed-state Monte Carlo simulations including diabatic transitions for the same Λ system. Dotted curve: the force $\bar{F}$ calculated for the two-level case with $\kappa_0=40\Gamma$ and $\delta=-2\Gamma$. Dash-dotted curve: dressed-state Monte Carlo simulations including diabatic transitions for the same two-level case.

From the calculations of the force, it is clear that the part of the force originating from transitions between the states $|a\rangle$ and $|b\rangle$ dominates in the whole velocity range. The force has, however, for small velocities the opposite sign of the force for the two-level case with $\kappa_0=40\Gamma$ and $\delta=-2\Gamma$ (see the dotted curve in Fig. 2). Hence, the third level that has been introduced makes a significant difference, even though the part of the force directly connected with the transition between $|b\rangle$ and $|c\rangle$ is negligible.

The physics behind the new stronger force can best be discussed in the dressed-state basis of a stationary atom, which in the RWA and in the $\{|a\rangle,|b\rangle,|c\rangle\}$ basis is given as the eigenvectors of the matrix

$$\begin{bmatrix} 0 & \kappa_{ab}(z) & \kappa_{cb}(z) \\ \kappa_{ab}(z) & \delta_{ab} & 0 \\ \kappa_{cb}(z) & 0 & \delta_{cb} \end{bmatrix} ,$$

$$\kappa_{ab}(z)=\kappa_{ab}\cos(kz), \quad \kappa_{cb}(z)=\kappa_{cb}\cos(kz+\phi) . \quad (4)$$

The admixture of the three states $|a\rangle$, $|b\rangle$, and $|c\rangle$ in the dressed states is shown together with the corresponding dressed-state energies in Fig. 3 for $\phi=0$ as a function of position in the standard waves. At the nodes of the electric fields the dressed states correspond just to the three bare atomic states, while in the antinodes, they correspond to highly mixed atomic states.

A naive calculation of the force by Monte Carlo simulations similar to the ones discussed in [13], involving only the radiation transition rates between the dressed states and with the instantaneous forces defined as minus the gradient of the dressed-energy curve the atom stays on, results in a spatially averaged force that is essentially zero for all velocities. This failure to reproduce the mean force $\bar{F}$ given in Fig. 2 must be due to the neglect of diabatic transitions between the dressed states (which especially occur at the avoided crossings) and the disregard of coherences. It is known that when diabatic transitions are taken into account, the equation of motion for the populations and coherences no longer separate [12] and Monte Carlo simulations dealing only with populations cannot be expected to be correct. In order to understand the *physical mechanisms* behind the force for the Λ system, we have, however, made Monte Carlo simulations based on the populations along, but introducing reasonable diabatic transition probabilities. The avoided cross-

ing between the dressed states $|2\rangle$ and $|3\rangle$ involves essentially only the two atomic states $|a\rangle$ and $|b\rangle$ and hence the formalism of Ref. [14] can be applied. In Ref. [14] the diabatic transitions were considered as Landau-Zener transitions [15] and the Landau-Zener factor P_{LZ} going into the S matrix for the diabatic transitions is given by

$$P_{\mathrm{LZ}}(v)=\exp[-2\pi\xi(v)], \quad \xi(v)=\frac{\delta_{ab}^2}{4k\kappa_{ab}v} \tag{5}$$

in our notation. If coherences are disregarded, P_{LZ} would be the transition probability between the two dressed states. In the Monte Carlo simulations, we have heuristically used this probability to decide whether the atom should change from one of the two involved dressed states to the other when the atom is just at the middle of the avoided crossing.

The other avoided crossing between the dressed states $|1\rangle$ and $|2\rangle$ cannot be treated in the Landau-Zener picture since if the coupling between the two dressed states is neglected, the potential curves would be two crossing curves: one constant and one with a parabolic shape in the region of interest instead of a single linear crossing, as needed in the Landau-Zener model. Simple analytical models for such a crossing as given in Ref. [16] cannot be applied in our case, due to the complicated spatial dependence of the interaction. However, to also include diabatic transition between $|1\rangle$ and $|2\rangle$ in the Monte Carlo simulations, we approximated the broad avoided crossing by a model with two initially degenerate curves coupled by a constant interaction matrix element. This model gives the following probability for an atom to change curve along the crossing [17]:

$$P_{\parallel}(v)=\sin^2\left[\frac{V_{12}\Delta l}{\hbar v}\right], \tag{6}$$

where V_{12} is the interaction energy matrix element between the two dressed states and Δl is the effective spatial extension of the interaction. $V_{12}\Delta l$ can be estimated by considering the dressed-state levels with and without the interaction present. In such a way we found that $V_{12}\Delta l/\hbar \sim \pi\Gamma/k$. The probability given by Eq. (6) with $V_{12}\Delta l/\hbar=\pi\Gamma/(2\kappa)$ has been introduced in the Monte Carlo simulations. In Fig. 2 the force calculated by this Monte Carlo method (dashed curve) is shown. The shape as well as the magnitude of the Monte Carlo force is very similar to $\bar{F}$ if the smaller structures are neglected. The

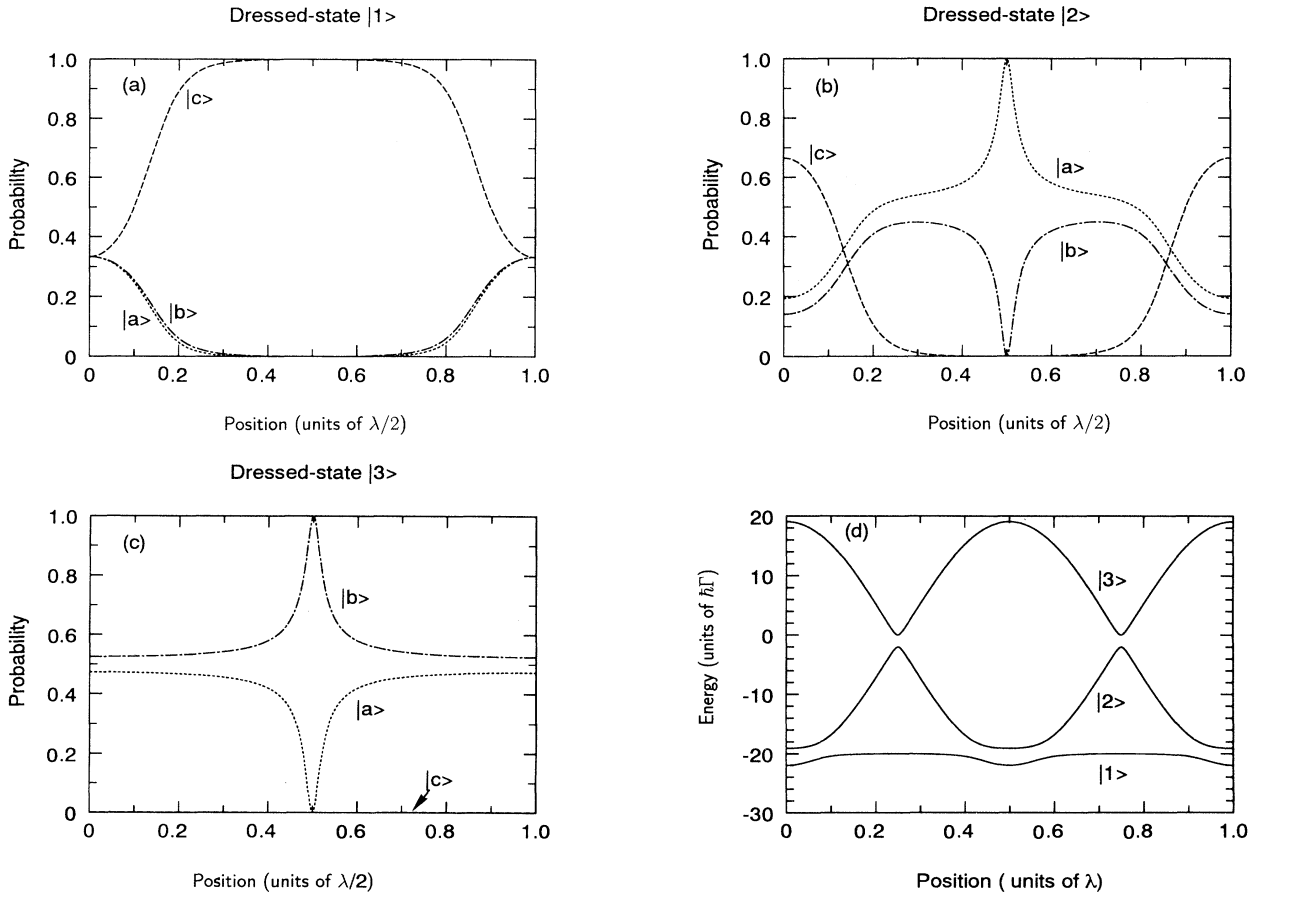

FIG. 3. (a) The probability of finding an atom in each of the three atomic states $|a\rangle$, $|b\rangle$, and $|c\rangle$ as a function of position in the standing wave when it is known that it is in the dressed-state $|1\rangle$. (b) Same as (a), but for the dressed state $|2\rangle$. (c) Same as (a), but for the dressed state $|3\rangle$. (d) The dressed-state energies. The standing-wave parameters are the same as in Fig. 2.

agreement is actually better than could be expected, since in the Monte Carlo approach the treatment of the diabatic transitions is nonexact and the coherences is disregarded. The fourth curve in Fig. 2 represents the two-level force calculated by Monte Carlo simulations, including the Landau-Zener probability given by Eq. (5) for the diabatic transitions. Here again the simplified model can explain most of the physics, but the magnitude of the force is, in this case, slightly below the spatial averaged force calculated by using the optical Bloch equations.

For an atomic velocity equal to Γ/k, both the diabatic transition probabilities are close to unity. The large decelerating force for velocities around this value can be understood by the following argument. Assume that the atom starts in the $|1\rangle$ state at the node of the standing wave. In this state, the force on the atom is small due to the nearly constant energy of the state. Furthermore, it is a relatively stable state since it is nearly the pure ground state $|c\rangle$ in the atomic basis. When the atom arrives at the antinode, it will jump (according to our model) to the $|2\rangle$ state and start losing kinetic energy as it climbs the potential for this state on its way toward the next node of the field. If a radiative decay occurs, the atom will preferentially fall back into the $|1\rangle$ state where the force is small. Otherwise, it will continue on the $|2\rangle$-state potential until the node and then make a diabatic transition to the $|3\rangle$ state, where it will continue to lose kinetic energy. In the $|3\rangle$ state, the atom still prefers to decay to the $|1\rangle$ state, where it will probably stay until the next antinode. By introducing a third level, one then partly avoids the problem in the two-level case with radiative decays to an accelerating potential.

The maximum spatially averaged force, which could hypothetically be obtained with the dressed states shown in Fig. 3(d), would arise if the atom between the antinode and node stayed in the $|2\rangle$ state and from the node to antinode would stay in the $|3\rangle$ state where it then decays radiatively back to the $|2\rangle$ state. This force is $\approx 13\,\hbar k\Gamma$, which is only a factor of ~ 5 larger than the maximum of $\bar{F}$ for the three-level case in Fig. 2, but about ten times higher than the maximum spatially averaged force obtainable for two-level atoms with the same laser intensity.

B. The momentum diffusion coefficient $\bar{D}$

The momentum diffusion coefficient $\bar{D}$ is shown in Fig. 4 for the same Λ system as considered above (solid curve) and for the two-level case with $\kappa_0=40\Gamma$ and $\delta=-2\Gamma$ (dashed curve). The velocity dependence of the momentum diffusion coefficient for the Λ system is very different from the two-level atom situation. First, $\bar{D}$ peaks at a nonzero velocity and has a local minimum at zero velocity. This is in contrast to the normal two-level situation (see Fig. 4, dashed curve), where the spatially averaged momentum diffusion coefficient is roughly a monotonically decreasing function of v. Calculations show that the reason for this low diffusion coefficient at low velocities is that the atom stays in the dressed state $|1\rangle$ most of the time and hence only feels a small nonfluctuating force (see Fig. 3). Second, the diffusion coefficient $\bar{D}$ is seen to be an order of magnitude smaller than in the corresponding two-level case. The effect of the special shape of the momentum diffusion coefficient on the steady-state momentum distribution will be discussed further in Sec. IV.

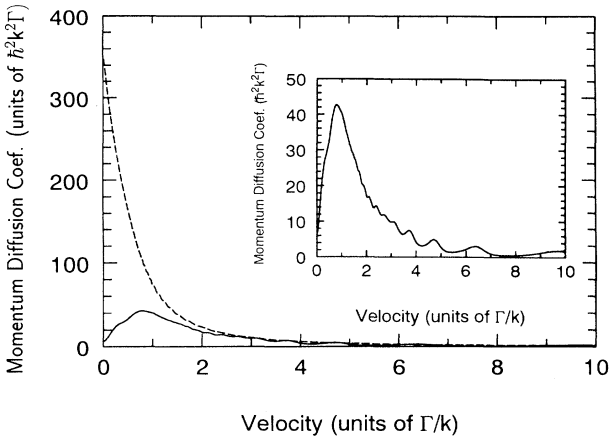

FIG. 4. The spatially averaged atomic momentum diffusion coefficient as a function of velocity. Solid curve: the Λ-system case with the standing wave parameters is the same as in Fig. 2 (see also the inset). Dashed curve: two-level case with $\kappa_0=40\Gamma$ and $\delta=-2\Gamma$.

III. DEPENDENCE ON THE RELATIVE DISPLACEMENT OF THE TWO STANDING WAVES

In order to optimize the cooling scheme, the relative displacement of the two standing waves, or, equivalently, the phase ϕ defined in Sec. II, has also been varied. In Fig. 5 the force at zero velocity F_0 is shown as a function of the phase ϕ for the same Rabi frequencies and laser detunings as in the Λ-system case discussed above. Only when $\phi=n\pi/2$, where n is an integer, the force vanishes at zero velocity. For all other phases, a finite force is present, as has been discussed theoretically and observed

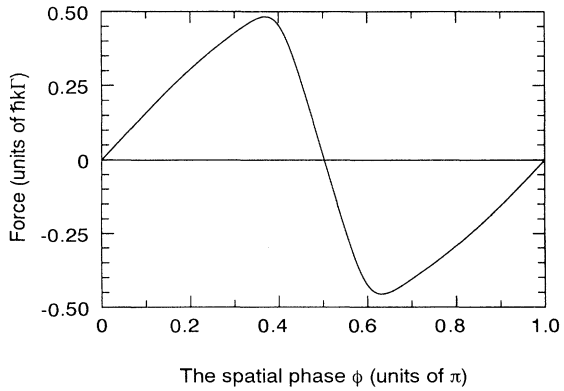

FIG. 5. The spatially averaged force F_0 at zero velocity as a function of the phase $\phi=k\Delta z$, where k is the norm of the wave vectors and Δz is the relative displacement of the nodes of the two standing waves. The Rabi frequencies and detunings are the same as in Fig. 2.

in experiments [6]. We have, for a set of phases, calculated the force and the momentum diffusion coefficient as a function of velocity, but even though cooling toward a finite velocity is possible for $\phi \neq n\pi/2$, the best cooling condition is obtained when $\phi = n\pi$. For $\phi = (n+\frac{1}{2})\pi$, the force is significantly smaller than for $\phi = n\pi$, which can be seen in Fig. 6, where the spatially averaged force $\bar{F}$ for $\phi = \pi/2$ is shown (solid curve) as a function of velocity. The corresponding dressed-state energies are shown in Fig. 7, where it should be noted that the coupling between the states $|1\rangle$ and $|2\rangle$ is much weaker than in Fig. 3. Hence we have performed a Monte Carlo simulation where the diabatic transition between the states $|1\rangle$ and $|2\rangle$ was neglected to calculate the force. This force is represented by the dashed curve in Fig. 6. Again the simple physical picture gives reasonable results. The structures in the Monte Carlo are due to the statistical nature of the calculations and have no physical significance.

IV. THE MOMENTUM DISTRIBUTION

In the case of two-level atoms moving in strong standing light waves, it has been found that the steady-state momentum distribution can be reasonably well expressed by [9,10,18,19]

$$f(p) = f(0)\exp\left[m\int_0^{p/m}\frac{\bar{F}(v')}{\bar{D}(v')}dv'\right] . \tag{7}$$

In Fig. 8 this steady-state momentum distribution is shown for the helium case considered in Sec. V below, together with distributions for fictitious atoms which have the same atomic properties as helium, except for the mass. Note that the scale on the horizontal axis is the atomic momentum divided by the square root of the mass. This means that atomic samples having the same steady-state energy distribution would have coinciding curves in Fig. 8. Even though the mean force and the momentum diffusion coefficient are quite different from those in the two-level atom case for low velocities, the steady-state distributions depend only weakly on the atomic mass as for two-level atoms.

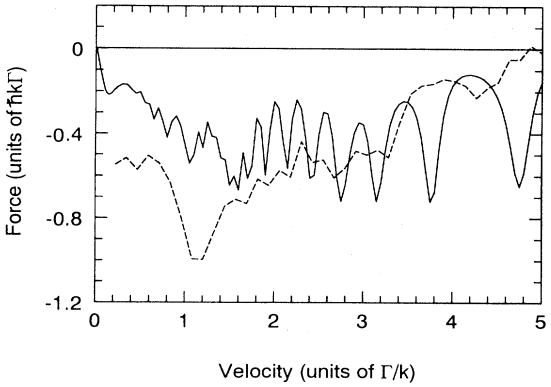

FIG. 6. The spatially averaged force acting on an atom moving in two standing waves with relative phase of $\pi/2$ and parameters as defined in Fig. 2. Solid curve: the spatially averaged force $\bar{F}$. Dashed curve: dressed-state Monte Carlo simulations.

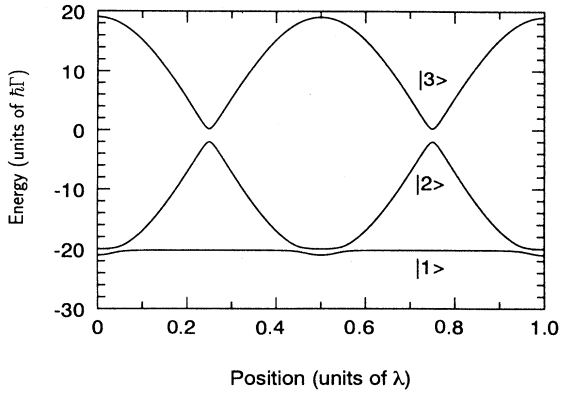

FIG. 7. Dressed-state energies for standing waves with a relative phase of $\pi/2$.

For a two-level atom moving in a standing light wave, the spatially averaged force can be approximated by

$$\bar{F}(v) = \frac{\alpha_F v}{1+(v/v_F)^2} \tag{8}$$

if the adiabatic condition

$$kv \ll (2\pi\delta^4/\kappa_0^2)^{1/3} \tag{9}$$

is fulfilled [12]. Here α_F is the friction coefficient and v_F a constant. In the same limit, the momentum diffusion coefficient can be written [9]

$$\bar{D}(v)\frac{D_0}{1+(v/v_D)^2} , \tag{10}$$

where D_0 is the diffusion coefficient at zero velocity and v_D is a constant. calculations show that $v_F \approx v_D$ for nearly all combinations of detunings and Rabi frequencies

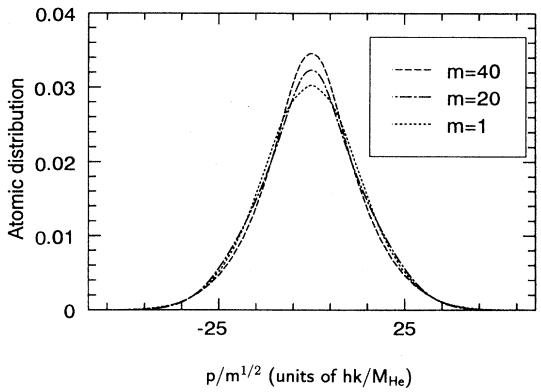

FIG. 8. Calculated atomic distributions from Eq. (7) with $\bar{F}(v)$ and $\bar{D}(v)$ given in Figs. 2 and 4. p is the momentum of the atom in the direction of the laser beams and m indicates the mass of the atom relative to helium. All other parameters are assumed to be like those for the $1s2s\ ^3S_1$ to $1s2p\ ^3P_1$ transition in helium (see Sec. V).

[20], so the steady-state momentum distribution can be found from Eq. (7) to be

$$f(p)=f(0)\exp\left[-\frac{\alpha_F}{D_0}\frac{p^2}{2m}\right]. \quad (11)$$

Equation (11) corresponds to a thermal distribution with $k_B T=D_0/\alpha_F$, where k_B is Boltzmann's constant and T the temperature. Plotted as a function of $p/m^{1/2}$, this distribution is clearly independent of the mass of the atoms.

V. EXPERIMENTAL REALIZATION

In this section, a realistic experimental realization of the Λ-system laser-cooling scheme considered above will be proposed. In helium, a closed cooling transition between the levels $1s2s\ ^3S_1$ and $1s2p\ ^3P_1$ exists at a wavelength of 1083 nm. Since the total quantum number $J=1$ for both states, transitions between the Zeeman sublevels with $M_J=0$ are forbidden. By applying two near-resonant standing waves, which are right and left circularly polarized, respectively, one can, after a short period of optical pumping, obtain an effective Λ system consisting of the Zeeman substates with $M_J=\pm 1$ of the lower-lying state and the substate with $M_J=0$ of the upper state. The decay rate of the upper state is the same for both states $M_J=\pm 1$ and will be denoted Γ. If a single elliptically polarized standing wave is created with the ratio of the intensity of the σ^+ and σ^- components given by $(\kappa_{ab}/\kappa_{cb})^2$ and a magnetic field is applied in the direction of the standing wave such that the Zeeman splitting between the two substates with $M_J=\pm 1$ is equal to $\delta_{ab}-\delta_{cb}=18\Gamma$, then if the laser frequency is detuned -11Γ with respect to the field-free transition, the laser-cooling situation discussed above can be obtained with the right choice of laser power. The Clebsch-Gordan coefficient of the two involved transitions differs by a sign, but the force and the momentum diffusion coefficient do not depend on the sign of the Rabi frequencies.

The present cooling scheme should also be applicable for Λ systems where bichromatic standing waves are needed as long as the relative frequency difference between the two laser frequencies is small and the atomic beam interacts with the light beams at a position where the relative node separation of the beams is close to zero. In all the calculations presented, spatially averaged quantities have been used and hence possible localization effects have been disregarded. Calculations have shown that the atom, when the velocity is low, stays most of the time in the dressed state $|1\rangle$ [see Fig. 3(d)]. The energy level of the $|1\rangle$ state changes only slightly as a function of position, which means that localization will only occur at very low velocities.

VI. DISCUSSION

In the presented laser-cooling scheme both laser beams were negatively detuned with respect to the involved transitions. This is different from the normal stimulated cooling situation with two-level atoms as well as from recently proposed cooling schemes of three-level atoms [2,3], where positively detuned light is used. The aim of the work presented in [2,3] has been to study the possibility of creating sub-Doppler cooled atomic samples, while the purpose of the present work has been to find good cooling conditions for large velocity ranges.

The laser-field intensities chosen above are somewhat arbitrary. Similar improvements in the cooling force compared to the two-level situation can be found for both higher and lower Rabi frequencies. The optimum choice of the Rabi frequencies and detunings is not easy to give. However, from our discussion in the dressed-state basis, it is clear that the main idea is to choose the detuning of the strong field small compared to the Rabi frequency in order to have high probabilities for Landau-Zener diabatic transitions. At the same time, the detuning of the weak laser beam should be negative with a size of the order of half the maximum Rabi frequency of the strong standing wave so the two lower-lying dressed states couple effectively at the antinodes of the standing waves. Generally, the ratio κ_{ab}/κ_{cb} can be small, which means that the additional power needed, compared to the two-level case, is not significant. We have also made calculations for three-level V systems, but if both a strong cooling force and a large velocity capture range are sought, a Λ system, as the one discussed above, seems to be the more favorable case.

VII. CONCLUSION

Laser cooling of atoms with three-level Λ configurations by using two negatively detuned standing light waves has been investigated. The basic physics behind the force acting on the atoms can be understood by using the dressed-atom picture. The strong obtainable force and the low momentum diffusion coefficient near zero velocity can be seen as the results of favorable diabatic transition between the dressed states as certain positions in space. The cooling scheme seems to be superior to the two-level stimulated-cooling situation with the same total laser intensity. It was found that the achievement of the cooling scheme depends on the relative phase between the two standing waves involved. Finally, a fairly simple implementation of the cooling scheme for the case of metastable helium atoms was proposed.

ACKNOWLEDGMENTS

The author would like to thank Klaus Mølmer for taking part in many fruitful and clarifying discussions. The critical but constructive reading of the manuscript by Tilman Pfau is appreciated. Financial support from the Carlsberg Foundation is gratefully acknowledged.

APPENDIX

In this appendix the equations necessary for calculating the force $F(z,v)$ acting on the atom and the momentum diffusion coefficient $D(z,v)$ as function of position and velocity are presented for the three-level Λ configuration shown in Fig. 1. The equations below have

been derived on the basis of [9], where the following conditions were imposed. First, the standing-wave light field is treated classically. Second, the velocity of the atom is assumed to be constant during its travel over several wavelengths. Third, the interacting time is assumed to be larger than a few times the lifetime of the excited state, so that any transient behavior can be neglected.

1. The force $F(z,v)$

Under the above conditions, the force F can be written as

$$F(z,v)=\mathrm{Tr}\{\Phi[W^0(z,v)]\} , \tag{A1}$$

where $W^0(z,v)$ is internal-state density matrix with the equation of motion given by

$$v\frac{dW^0(z,v)}{dz}=B[W^0(z,v)] \tag{A2}$$

and the operators Φ and B in the basis of the atomic states $|a\rangle$, $|b\rangle$, and $|c\rangle$ (see Fig. 1) are given by

$$(\Phi[V])_{aa}=-\tfrac{1}{4}\hbar k\kappa_{ab}\sin(kz)(V_{ab}+V_{ba}) , \tag{A3a}$$

$$(\Phi[V])_{bb}=-\tfrac{1}{4}\hbar k[\kappa_{ab}\sin(kz)(V_{ab}+V_{ba}) +\kappa_{cb}\sin(kz+\phi)(V_{cb}+V_{bc})] , \tag{A3b}$$

$$(\Phi[V])_{cc}=-\tfrac{1}{4}\hbar k\kappa_{cb}\sin(kz+\phi)(V_{cb}+V_{bc}) , \tag{A3c}$$

$$(\Phi[V])_{ab}=-\tfrac{1}{4}\hbar k[\kappa_{ab}\sin(kz)(V_{aa}+V_{bb}) +\kappa_{cb}\sin(kz+\phi)V_{ac}] , \tag{A3d}$$

$$(\Phi[V])_{ac}=-\tfrac{1}{4}\hbar k[\kappa_{ab}\sin(kz)V_{bc}+\kappa_{cb}\sin(kz+\phi)V_{ab}] , \tag{A3e}$$

$$(\Phi[V])_{cb}=-\tfrac{1}{4}\hbar k[\kappa_{cb}\sin(kz+\phi)(V_{cc}+V_{bb}) +\kappa_{ab}\sin(kz)V_{ca}] , \tag{A3f}$$

$$(\Phi[V])_{ba}=\{(\Phi[V])_{ab}\}^* , \tag{A3g}$$

$$(\Phi[V])_{ca}=\{(\Phi[V])_{ac}\}^* , \tag{A3h}$$

$$(\Phi[V])_{bc}=\{(\Phi[V])_{cb}\}^* , \tag{A3i}$$

and

$$(B[V])_{aa}=\Gamma_{ab}V_{bb}(z) +\tfrac{1}{2}i\kappa_{ab}\cos(kz)[V_{ba}(z)-V_{ab}(z)] , \tag{A4a}$$

$$(B[V])_{bb}=-(\Gamma_{ab}+\Gamma_{cb})V_{bb}(z) +\tfrac{1}{2}i\kappa_{cb}\cos(kz+\phi)[V_{cb}(z)-V_{bc}(z)] , +\tfrac{1}{2}i\kappa_{ab}\cos(kz)[V_{ab}(z)-V_{ba}(z)] \tag{A4b}$$

$$(B[V])_{cc}=\Gamma_{cb}V_{bb}(z) +\tfrac{1}{2}i\kappa_{cb}\cos(kz+\phi)[V_{bc}(z)-V_{cb}(z)] , \tag{A4c}$$

$$(B[V])_{ab}=-\left[\frac{\Gamma_{ab}}{2}+\frac{\Gamma_{cb}}{2}+i\delta_{ab}\right]V_{ab}(z) +\tfrac{1}{2}i\kappa_{ab}\cos(kz)[V_{bb}(z)-V_{aa}(z)] -\tfrac{1}{2}i\kappa_{cb}\cos(kz+\phi)V_{ac}(z) , \tag{A4d}$$

$$(B[V])_{ac}=-i(\delta_{ab}-\delta_{cb})V_{ac}(z) -\tfrac{1}{2}i\kappa_{cb}\cos(kz+\phi)V_{ab}(z) +\tfrac{1}{2}i\kappa_{ab}\cos(kz)V_{bc}(z) , \tag{A4e}$$

$$(B[V])_{cb}=-\left[\frac{\Gamma_{cb}}{2}+\frac{\Gamma_{ab}}{2}+i\delta_{cb}\right]V_{cb}(z) +\tfrac{1}{2}i\kappa_{cb}\cos(kz+\phi)[V_{bb}(z)-V_{cc}(z)] -\tfrac{1}{2}i\kappa_{ab}\cos(kz)V_{ca}(z) , \tag{A4f}$$

$$(B[V])_{ba}=\{(B[V])_{ab}\}^* , \tag{A4g}$$

$$(B[V])_{ca}=\{(B[V])_{ac}\}^* , \tag{A4h}$$

$$(B[V])_{bc}=\{(B[V])_{cb}\} . \tag{A4i}$$

Here κ_{ab} is the maximum Rabi frequency of the laser-induced coupling between the states $|a\rangle$ and $|b\rangle$, $\delta_{ab}=\omega_L-\omega_{ab}$ (where ω_L is the laser angular frequency and ω_{ab} is the angular frequency of the transition $|b\rangle\rightarrow|a\rangle$) is the laser detuning, and Γ_{ab} is the decay rate of the state $|b\rangle$ toward the state $|a\rangle$, κ_{cb}, δ_{cb}, and Γ_{cb} are the same quantities, but for the transition between the states $|b\rangle$ and $|c\rangle$. $\phi=k\Delta z$, where k is the norm of the wave vectors and Δz is the relative displacement of the nodes of the two standing waves.

2. The momentum diffusion coefficient $D(z,v)$

The momentum diffusion coefficient $D(z,v)$ can be written as

$$D(z,v)=\mathrm{Tr}\{\Phi[\tilde{W}^1(z,v)]\}+\gamma_{\mathrm{SE}}(z,v) \tag{A5}$$

with

$$\tilde{W}^1(z,v)\equiv W^1(z,v)-\mathrm{Tr}[W^1(z,v)]W^0(z,v) \tag{A6}$$

and with the equation of motion of $W^1(z,v)$ given by

$$v\frac{dW^1(z,v)}{dz}=B[W^1(z,v)]+\phi[W^0(z,v)] . \tag{A7}$$

The term γ_{SE} is the contribution from spontaneously emitted photons to the momentum diffusion coefficient and can generally be written

$$\gamma_{\mathrm{SE}}(z,v)=\alpha(\Gamma_{ab}+\Gamma_{cb})(\hbar k)^2W^0_{ee}(z,v) , \tag{A8}$$

where α is a positive quantity that depends on the spontaneous-emission pattern of the excited state, but will always be smaller than 0.5. In the calculations presented, α was chosen to be 0.5, i.e., the calculated diffusion coefficient is generally slightly higher than in a real situation.

[1] P. Lett, R. Watts, C. Westbrook, W. D. Phillips, P. Gould, and H. Metcalf, Phys. Rev. Lett. **61**, 169 (1988); Y. Shevy, D. S. Weiss, P. J. Ungar, and S. Chu, *ibid.* **62**, 1118 (1989); J. Dalibard, C. Salomon, A. Aspect, E. Arimondo, R. Kaiser, N. Vansteenkiste, and C. Cohen-Tannoudji, in *Proceedings of the 11th Conference on Atomic Physics,* edited by S. Haroche, J. C. Gay, and G. Grynberg (World Scientific, Singapore, 1989); S. Chu, D. S. Weiss, Y. Shevy, and P. J. Ungar, in *Proceedings of the 11th Conference on Atomic Physics, ibid.*

[2] R. Gupta, C. Xie, S. Padua, H. Batelaan, and H. Metcalf, Phys. Rev. Lett. **71**, 3087 (1993).

[3] C. A. Sackett, J. Chen, J. J. Tollet, and R. G. Hulet (unpublished).

[4] A. Aspect, E. Arimondo, R. Kaiser, N. Vansteenkiste, and C. Cohen-Tannoudji, Phys. Rev. Lett. **61**, 826 (1988); J. Opt. Soc. Am. B **6**, 2112 (1989); F. Mauri, F. Papoff, and E. Arimondo, in *Proceedings of the Light Induced Kinetic Effects,* edited by L. Moi *et al.* (Ets Editrice, Pisa, 1991), p. 89; M. A. Ol'shanii and V. G. Minogin, in *Proceedings of the Light Induced Kinetic Effects, ibid.*, p. 99; M. G. Prentiss, N. P. Bigelow, M. S. Shahriar, and P. R. Hemmer, Opt. Lett. **16**, 1695 (1991); P. R. Hemmer, M. G. Prentiss, M. S. Shahriar, and N. P. Bigelow, Opt. Commun. **89**, 335 (1992).

[5] J. Javanainen, Phys. Rev. Lett. **64**, 529 (1990); R. Grimm, Yu. Ovchinnikov, A. I. Sidorov, and V. S. Letokhov, *ibid.* **65**, 1415 (1990); A. I. Sidorov, R. Grimm, and V. S. Letokhov, J. Phys. B **24**, 3733 (1991); Yu. B. Ovchinnikov, A. I. Sidorov, R. Grimm, and V. S. Letokhov, *ibid.* **24**, L539 (1991); R. Grimm, Yu. Ovchinnikov, A. I. Sidorov, and V. S. Letokhov, Opt. Commun. **84**, 18 (1991); J. Söding, R. Grimm, J. Kowalski, Yu. Ovchinnikov, and A. I. Sidorov, Europhys. Lett. **20**, 101 (1992); P. R. Hemmer, M. S. Shahriar, M. G. Prentiss, D. P. Katz, K. Berggren, J. Mervis, and N. P. Bigelow, Phys. Rev. Lett. **68**, 3148 (1992).

[6] T. Pfau, C. S. Adams, and J. Mlynek, Europhys. Lett. **21**, 439 (1993); C. S. Adams, T. Pfau, Ch. Kurtsiefer, and J. Mlynek, Phys. Rev. A **48**, 2108 (1993); T. Pfau, Ch. Kurtsiefer, C. S. Adams, M. Sigel, and J. Mlynek, Phys. Rev. Lett. **71**, 3427 (1993).

[7] S. Chang, B. M. Garraway, and V. G. Minogin, Opt. Commun. **77**, 19 (1990).

[8] D. Wineland and W. Itano, Phys. Rev. A **20**, 1521 (1979); V. S. Letokhov and V. G. Minogin, Phys. Rep. **73**, 1 (1981).

[9] K. Berg-Sørensen, Y. Castin, E. Bonderup, and K. Mølmer, J. Phys. B **25**, 4195 (1992).

[10] R. G. DeVoe, Opt. Lett. **20**, 1605 (1991).

[11] M. Drewsen and N. V. Vitanov, J. Phys. B **26**, 4109 (1993).

[12] J. Dalibard and C. Cohen-Tannoudji, J. Opt. Soc. Am. B **2**, 1707 (1985).

[13] J. Dalibard, A. Heidmann, C. Salomon, A. Aspect, H. Metcalf, and C. Cohen-Tannoudji, in *Fundamentals of Quantum Optics II,* edited by F. Ehlotzky (Springer, Berlin, 1987).

[14] K. Mølmer, Phys. Scr. **45**, 246 (1992).

[15] C. Zener, Proc. R. Soc. London Ser. A **137**, 696 (1932); E. E. Nikitin and S. Ya. Umanski, *Theory of Slow Atomic Collisions* (Springer, Berlin, 1984).

[16] K.-A. Suominen, Opt. Commun. **93**, 126 (1992).

[17] See, e.g., B. W. Shore, *The Theory of Coherent Atomic Excitation* (Wiley, New York, 1990).

[18] M. Drewsen, Ph.D. Thesis, Aarhus University, 1994.

[19] K. Mølmer (unpublished).

[20] K. Berg-Sørensen and K. Mølmer (private communication).